

Radiation and Chemical Reaction Effects on MHD Flow of Continuously Moving Vertical Surface with Heat and Mass Transfer through Porous Medium with Ohmic Heating

K.Laxmaiah¹, M.Chenna Krishna Reddy²

¹Department of Mathematics, Guru Nanak Institutions Technical Campus, Ibrahimpatnam, Ranga Reddy, Telangana – 501 506.

²Department of Mathematics, Osmania University, Hyderabad, Telangana – 500 007

Abstract:- The aim of the present chapter is radiation and viscous dissipation effect to MHD flow with heat and mass transfer from a vertical surface in presence of Ohmic heating, chemical reaction and viscous dissipation has been presented. The governing equations of the momentum, thermal and concentration fields are solved by perturbation technique. The velocity, temperature, concentration and skin friction have been evaluated for variation in the different governing parameters by graphically.

Keywords: Chemical reaction, Heat generation, Radiation and Ohmic Heating

INTRODUCTION

Nowadays, the period of MHD is of great enlargement and differentiation of subject matter. These problems have attracted the interest of many investigators because of their application in liquid metals, electrolytes and ionized gases. The problem of heat and mass transfer along a vertical plate with variable temperature and concentration in the presence of magnetic field has been studied by Elbashbeshy [5]. Hossain and Rees [9] have studied effect of combined heat and mass transfer in natural convection flow from a vertical wavy surface. Chien-Hsin-Chen [3] has analyzed combined heat and mass transfer in MHD free convection from a vertical surface with ohmic heating and viscous dissipation. Hall current on fluid flow with concentration plays an important role in MHD power generation, in various meteorological and astrophysical studies and in plasma flow through magnetohydrodynamic power generators. Keeping in view of all these facts, a number of researchers have studied the Hall current effect on free and forced convective flows. Acharya et al. [11], Aboeldahab and Elbarbary [6], Datta and Jana [13] have studied the effect of Hall current on MHD flow with heat and mass transfer. Hossain et al. [10] have investigated the effect of radiation on free convection from a porous vertical plate. The radiation effect on MHD free convection flow of a gas at a stretching surface with a uniform free stream has been analyzed by Ghaly and Elbarbary [2]. Muthukumarswamy and Senthil [20] have studied the effects of heat and mass transfer on moving vertical plate in the presence of thermal radiation. In all the above investigations, the combined effect of ohmic heating and viscous dissipation are not analyzed. Hossain [8] has studied the effects of viscous and Joule heating on free convective MHD flow with variable plate temperature. Babu and Reddy [22] have analyzed the mass transfer effects on MHD mixed convective flow from a vertical surface with ohmic heating and viscous dissipation. Ganesan and Palani [17] have investigated the numerical solution of unsteady MHD flow past a semi-infinite isothermal vertical plate. Ganesan and Palani [16] have also presented a finite difference analysis of unsteady natural convection MHD flow past an inclined plate with variable surface heat and mass flux. Aydin and Kaya [14] have analyzed the non-Darcian forced convection flow of viscous dissipating fluid over a flat plate embedded in a porous medium. Aydin and Kaya [15] have also studied MHD mixed convection of a viscous dissipating fluid about permeable vertical flat plate. Rita Choudhury and Sajal Kumar Das [21] Mixed Convective Visco-Elastic MHD Flow with Ohmic Heating.

In many chemical engineering processes, the chemical reaction do occur between mass and fluid in which plate is moving. These processes take place in numerous industrial applications such as polymer production, manufacturing of ceramics or glassware and food processing. In the light of the fact that, the combination of heat and mass transfer problems with chemical reaction are of importance in many processes, and have, therefore received a considerable amount of attention in recent years. In processes such as drying, evaporation at the surface of a water body, energy transfer in a wet cooling tower and the flow a desert cooler, heat and mass transfer occur simultaneously. Possible applications of this type of flow can be found in many industries. For example, in the power industry, among the methods of generating electricity is one in which electrical energy is extracted directly from the moving conducting fluid. Chamkha [1] studied the MHD flow of a numerical of uniformly stretched vertical permeable surface in the presence of heat generation/absorption and a chemical reaction. Muthucumarswamy and Ganesan [19] investigated the effects of a chemical reaction on the unsteady flow past an impulsively started semi-infinite vertical plate, which subjected to uniform heat flux. Ibrahim et.al. [7] Analyzed the effects of the chemical reaction and radiation absorption on the unsteady MHD free convection flow past a semi- infinite vertical permeable moving plate with heat source and suction. Mohamed

[18] has discussed double-diffusive convection radiation interaction on unsteady MHD flow over a vertical moving porous plate with heat generation and Soret effects, Ch Kesavaiah et.al [4] has effects of the chemical reaction and radiation absorption on an unsteady MHD convective heat and mass transfer flow past a semi-infinite vertical permeable moving plate embedded in a porous medium with heat source and suction, Bhavana et.al [12] considered the Soret effect on free convective unsteady MHD flow over a vertical plate with heat source.

The present chapter is radiation and viscous dissipation effect to MHD flow with heat and mass transfer from a vertical surface in presence of Ohmic heating, chemical reaction and viscous dissipation has been presented. The governing equations of the momentum, thermal and concentration fields are solved by perturbation technique. The velocity, temperature, concentration and skin friction have been evaluated for variation in the different governing parameters by graphically.

I. MATHEMATICAL FORMULATION

We consider the steady, two-dimensional laminar, incompressible flow of a chemically reacting, viscous fluid on a continuously moving vertical surface in the presence of a uniform magnetic field, radiation absorption with heat generation, uniform heat and mass flux effects issuing a slot and moving with uniform velocity in a fluid at rest. Let the x-axis be taken along the direction of motion of the surface in the upward direction and y-axis is normal to the surface. The temperature and concentration levels near the surface are raised uniformly. The induced magnetic field, viscous dissipation is assumed to be neglected. Now, under the usual Boussinesq's approximation, the flow field is governed by the following equations.

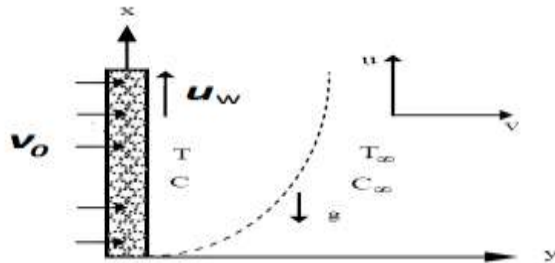


Figure (1): Flow configuration and coordinate system

Continuity equation

$$\frac{\partial u}{\partial x} + \frac{\partial v}{\partial y} = 0 \tag{1}$$

Momentum equation

$$u \frac{\partial u}{\partial x} + v \frac{\partial u}{\partial y} = g\beta(T - T_\infty) + g\beta^*(C - C_\infty) + \nu \frac{\partial^2 u}{\partial y^2} - \frac{\sigma B_0^2}{\rho} u - \frac{\nu}{K_p} u \tag{2}$$

Energy equation

$$\rho C_p \left(u \frac{\partial T'}{\partial x} + v \frac{\partial T'}{\partial y} \right) = k \frac{\partial^2 T'}{\partial y^2} + \mu \left(\frac{\partial u}{\partial y} \right)^2 - \frac{\partial q_r}{\partial y} + \sigma B_0^2 u^2 \tag{3}$$

$$u \frac{\partial C'}{\partial x} + v \frac{\partial C'}{\partial y} = D_M \frac{\partial^2 C'}{\partial y^2} - Kr'(C - C_\infty) \tag{4}$$

The relevant boundary conditions are

$$u = u_w, v = -v_0 = \text{const} < 0$$

$$\frac{\partial T}{\partial y} = -\frac{q}{k}, \quad \frac{\partial C}{\partial y} = -\frac{j''}{D} \quad \text{at } y = 0 \quad (5)$$

$$u \rightarrow 0, T \rightarrow T_\infty, C \rightarrow C_\infty \quad \text{as } y \rightarrow \infty$$

The radiative heat flux q_r is given by equation (5) in the spirit of Cogley et.al [15]

$$\frac{\partial q_r}{\partial y} = 4(T' - T'_\infty)I \quad \text{where } I = \int_0^\infty K_{\lambda w} \frac{\partial e_{b\lambda}}{\partial T^*} d\lambda,$$

$K_{\lambda w}$ – is the absorption coefficient at the wall and $e_{b\lambda}$ – is Planck's function, I is absorption coefficient

In order to write the governing equations and the boundary conditions the following non dimensional quantities are introduced.

$$u = \frac{u}{u_w}, Y = \frac{yv_0}{\nu}, T = \frac{T' - T'_\infty}{\left(\frac{qv}{kv_0}\right)}, C = \frac{C' - C'_\infty}{\left(\frac{j''v}{kv_0}\right)}, K = \frac{K_p v_0^2}{\nu^2}, M = \frac{\sigma B_0^2 \nu}{\rho v_0^2}$$

$$\text{Pr} = \frac{\mu C_p}{k}, Kr = \frac{Kr'v}{v_0^2}, Q_l = \frac{Q_l' j''v}{qv_0^2 \rho C_p}, Gr = \frac{\nu g \beta \left(\frac{qv}{kv_0}\right)}{u_w v_0^2} \quad (6)$$

$$Gc = \frac{\nu g \beta^* \left(\frac{j''v}{kv_0}\right)}{u_w v_0^2}, Ec = \frac{v_0^2}{C_p (T' - T'_\infty)}, R = \frac{4qvI}{kv_0}, Sc = \frac{\nu}{D_M}$$

Where u, v are the velocity along the x, y -axis, is constant obtained after integration conservation of mass in pre-non dimensional form not mentioned, ν is the kinematic viscosity, g is the acceleration due to gravity, T' is the temperature of the fluid, is the coefficient of volume expansion, C_p is the specific heat at constant pressure, is a constant, σ is the Stefan-Boltzmann constant, T'_w exceeds the free steam temperature T'_∞ , C' is the species concentration, is the wall temperature, C'_w is the concentration at the plate, T'_∞ is the free steam temperature far away from the plate, C'_∞ is the free steam concentration in fluid far away from the plate, k is the thermal conductivity of the fluid, B_0 is uniform magnetic field strength. It is a measure of the effect of flow on the magnetic field. The term $Q_0(T' - T'_\infty)$ is assumed to be the amount of heat generated or absorbed per unit volume. Q_0 is constant, which may take on either positive or negative values.

SOLUTION OF THE PROBLEM

In view of (6) the equations (2), (3) and (4) are reduced to the following non-dimensional form

$$\frac{d^2 U}{dY^2} + \frac{dU}{dY} - \left(M + \frac{1}{K}\right)U = -GrT - GcC \quad (7)$$

$$\frac{d^2 T}{dY^2} + \text{Pr} \frac{dT}{dY} + Ec \left(\frac{dU}{dY}\right)^2 - R \text{Pr} T = -Ec \text{Pr} MU^2 \quad (8)$$

$$\frac{d^2C}{dY^2} + Sc \frac{dC}{dY} - KrScC = 0 \quad (9)$$

The corresponding boundary conditions can be written as

$$\begin{aligned} U = 1, \quad \frac{\partial T}{\partial Y} = -1, \quad \frac{\partial C}{\partial Y} = -1 \quad \text{at } Y = 0 \\ U \rightarrow 0, T \rightarrow 0, C = 0 \quad \text{as } Y \rightarrow \infty \end{aligned} \quad (10)$$

where Gr is the thermal Grashof number, Gc is the solutal Grashof number, Pr is the fluid Prandtl number, Sc is the Schmidt number, Kr is the chemical reaction, Q is heat source parameter, Ec is the Eckert number, M is the magnetic field parameter and K is porosity parameter

The physical variables u, θ and C can be expanded in the power of Eckert number (Ec). This can be possible physically as Ec for the flow of an incompressible fluid is always less than unity. It can be interpreted physically as the flow due to the Joules dissipation is super imposed on the main flow. Hence we can assume

$$\begin{aligned} U(y) &= U_0(y) + EcU_1(y) + O(E^2) \\ T(y) &= T_0(y) + EcT_1(y) + O(E^2) \\ C(y) &= C_0(y) + EcC_1(y) + O(E^2) \end{aligned} \quad (11)$$

Using equation (11) in equations (7) – (9) and equating the coefficient of like powers of Ec , we have

$$\frac{d^2U_0}{dY^2} + \frac{dU_0}{dY} - \left(M + \frac{1}{K}\right)U_0 = -GrT_0 - GcC_0 \quad (12)$$

$$\frac{d^2T_0}{dY^2} + Pr \frac{dT_0}{dY} - RPrT_0 = -Ec \left(\frac{dU_0}{dY}\right)^2 - EcPrMU_0^2 \quad (13)$$

$$\frac{d^2C_0}{dY^2} + Sc \frac{dC_0}{dY} - KrScC_0 = 0 \quad (14)$$

$$\frac{d^2U_1}{dY^2} + \frac{dU_1}{dY} - \left(M + \frac{1}{K}\right)U_1 = -GrT_1 - GcC_1 \quad (15)$$

$$\frac{d^2T_1}{dY^2} + Pr \frac{dT_1}{dY} - RPrT_1 = -Pr \left(\frac{dU_0}{dY}\right)^2 - PrMU_0^2 \quad (16)$$

$$\frac{d^2C_1}{dY^2} + Sc \frac{dC_1}{dY} - KrScC_1 = 0 \quad (17)$$

and the corresponding boundary conditions are

$$\begin{aligned}
 U_0 = 1, T_0' = -1, C_0' = -1, U_1 = 0, T_1' = 0, C_1' = 0 \quad y = 0 \\
 U_0 \rightarrow 0, T_0' \rightarrow 0, C_0' \rightarrow 0, U_1 \rightarrow 0, T_1' \rightarrow 0, C_1' \rightarrow 0 \quad y \rightarrow \infty
 \end{aligned}
 \tag{18}$$

Solving equations (12) to (17) with the help of (18), we get

$$U_0 = A_1 e^{m_6 y} + A_2 e^{m_2 y} + A_3 e^{m_8 y}$$

$$T_0 = -\frac{1}{m_6} e^{m_6 y}$$

$$C_0 = -\frac{1}{m_2} e^{m_2 y}$$

$$\begin{aligned}
 U_1 = A_4 e^{m_{10} y} + A_5 e^{2m_8 y} + A_6 e^{2m_6 y} + A_7 e^{2m_2 y} + A_8 e^{(m_6+m_8)y} + A_9 e^{(m_2+m_8)y} + A_{10} e^{(m_2+m_8)y} \\
 + A_{11} e^{2m_8 y} + A_{12} e^{2m_6 y} + A_{13} e^{2m_2 y} + A_{14} e^{(m_6+m_8)y} + A_{15} e^{(m_2+m_8)y} + A_{16} e^{(m_2+m_8)y}
 \end{aligned}$$

$$\begin{aligned}
 T_1 = B_{13} e^{m_{10} y} + B_1 e^{2m_8 y} + B_2 e^{2m_6 y} + B_3 e^{2m_2 y} + B_4 e^{(m_6+m_8)y} + B_5 e^{(m_2+m_8)y} + B_6 e^{(m_2+m_8)y} \\
 + B_7 e^{2m_8 y} + B_8 e^{2m_6 y} + B_9 e^{2m_2 y} + B_{10} e^{(m_6+m_8)y} + B_{11} e^{(m_2+m_6)y} + B_{12} e^{(m_2+m_8)y}
 \end{aligned}$$

$$C_1 = 0$$

We get the following analytical solutions for the velocity, temperature and concentration

$$\begin{aligned}
 U = A_1 e^{m_6 y} + A_2 e^{m_2 y} + A_3 e^{m_8 y} + Ec \{ A_4 e^{m_{10} y} + A_5 e^{2m_8 y} + A_6 e^{2m_6 y} + A_7 e^{2m_2 y} + A_8 e^{(m_6+m_8)y} \\
 + A_9 e^{(m_2+m_8)y} + A_{10} e^{(m_2+m_8)y} + A_{11} e^{2m_8 y} + A_{12} e^{2m_6 y} + A_{13} e^{2m_2 y} + A_{14} e^{(m_6+m_8)y} \\
 + A_{15} e^{(m_2+m_8)y} + A_{16} e^{(m_2+m_8)y} \}
 \end{aligned}$$

$$\begin{aligned}
 T = -\frac{1}{m_6} e^{m_6 y} + Ec \{ B_{13} e^{m_{10} y} + B_1 e^{2m_8 y} + B_2 e^{2m_6 y} + B_3 e^{2m_2 y} + B_4 e^{(m_6+m_8)y} + B_5 e^{(m_2+m_8)y} \\
 + B_6 e^{(m_2+m_8)y} + B_7 e^{2m_8 y} + B_8 e^{2m_6 y} + B_9 e^{2m_2 y} + B_{10} e^{(m_6+m_8)y} + B_{11} e^{(m_2+m_6)y} + B_{12} e^{(m_2+m_8)y} \} \\
 C = -\frac{1}{m_2} e^{m_2 y}
 \end{aligned}$$

The computed solution for the velocity is valid at some distance from the slot, even though suction is applied from the slot onward. This is due to the assumption that velocity field is independent of the distance parallel to the plate. The fluids considered in this study are air (Pr = 0.71) and water (Pr = 7.0).

Skin friction

$$\begin{aligned}
 \tau = \left(\frac{\partial U}{\partial y} \right)_{y=0} \\
 = m_6 A_1 + m_2 A_2 + m_8 A_3 + Ec \{ m_{10} A_4 + 2m_8 A_5 + 2m_6 A_6 + 2m_2 A_7 + (m_6 + m_8) A_8 + (m_2 + m_8) A_9 \\
 + (m_2 + m_8) A_{10} + 2m_8 A_{11} + 2m_6 A_{12} + 2m_2 A_{13} + (m_6 + m_8) A_{14} + (m_2 + m_8) A_{15} + (m_2 + m_8) \}
 \end{aligned}$$

Nusselt number

$$Nu = \left(\frac{\partial T}{\partial y} \right)_{y=0}$$

$$= -1 + Ec \{ m_{10} B_{13} + 2m_8 B_1 + 2m_6 B_2 + 2m_2 B_3 + (m_2 + m_6) B_4 + (m_2 + m_8) B_5 + (m_2 + m_8) B_6$$

$$+ 2m_8 B_7 + 2m_6 B_8 + 2m_2 B_9 + (m_6 + m_8) B_{10} + (m_2 + m_6) B_{11} + (m_2 + m_8) B_{12} \}$$

Sherwood number

$$Sh = \left(\frac{\partial C}{\partial y} \right)_{y=0} = -1$$

II. APPENDIX

$$m_2 = m_4 = - \left(\frac{Sc + \sqrt{Sc^2 + 4KrSc}}{2} \right) m_6 = m_{10} = - \left(\frac{Pr + \sqrt{Pr^2 + 4RPr}}{2} \right) m_8 = m_{12} = - \left(\frac{1 + \sqrt{1 + 4\beta}}{2} \right)$$

$$\beta = \left(M + \frac{1}{K} \right) B_1 = - \frac{Pr m_8^2 A_3^2}{4m_8^2 + 2m_8 - RPr}$$

$$B_2 = - \frac{Pr m_6^2 A_1^2}{4m_6^2 + 2m_6 - RPr} B_3 = - \frac{Pr m_2^2 A_2^2}{4m_2^2 + 2m_2 - RPr} B_4 = - \frac{2Pr m_6 m_8 A_1 A_3}{(m_6 + m_8)^2 + Pr(m_6 + m_8) - RPr}$$

$$B_5 = - \frac{2Pr m_2 m_8 A_1 A_2}{(m_2 + m_6)^2 + Pr(m_2 + m_6) - RPr}$$

$$B_6 = - \frac{2Pr m_2 m_8 A_3 A_2}{(m_2 + m_8)^2 + Pr(m_2 + m_8) - RPr}$$

$$B_7 = - \frac{Pr MA_3^2}{4m_8^2 + 2m_8 - RPr} B_8 = - \frac{Pr MA_1^2}{4m_6^2 + 2m_6 - RPr} B_9 = - \frac{Pr MA_2^2}{4m_2^2 + 2m_2 - RPr}$$

$$B_{10} = - \frac{2Pr MA_1 A_3}{(m_6 + m_8)^2 + Pr(m_6 + m_8) - RPr} B_{11} = - \frac{2Pr MA_1 A_2}{(m_2 + m_6)^2 + Pr(m_2 + m_6) - RPr}$$

$$B_{12} = - \frac{2Pr MA_2 A_3}{(m_2 + m_8)^2 + Pr(m_2 + m_8) - RPr}$$

$$B_{13} = - \frac{1}{m_{10}} [2B_1 m_8 + 2B_2 m_6 + 2B_3 m_2 + 2B_4 (m_6 + m_8) + 2B_5 (m_2 + m_8) + 2B_6 (m_2 + m_8) + 2B_7 m_8$$

$$+ 2B_8 m_6 + 2B_9 m_2 + 2B_{10} (m_6 + m_8) + 2B_{11} (m_2 + m_6) + 2B_{12} (m_2 + m_8)]$$

$$A_1 = - \frac{Gr}{m_6 [m_6^2 + m_6 - \beta]} A_2 = - \frac{Gr}{m_2 [m_2^2 + m_2 - \beta]}$$

$$A_3 = (1 - A_1 - A_2) A_4 = - \frac{Gr B_{13}}{m_{10}^2 + m_{10} - \beta} A_5 = - \frac{Gr B_1}{4m_8^2 + 4m_8 - \beta}$$

$$A_6 = -\frac{GrB_2}{4m_6^2 + 4m_6 - \beta} \quad A_7 = -\frac{GrB_3}{4m_2^2 + 4m_2 - \beta} \quad A_8 = -\frac{GrB_4}{(m_6 + m_8)^2 + (m_6 + m_8) - \beta}$$

$$A_9 = -\frac{GrB_5}{(m_2 + m_8)^2 + (m_2 + m_8) - \beta} \quad A_{10} = -\frac{GrB_6}{(m_2 + m_8)^2 + (m_2 + m_8) - \beta}$$

$$A_{11} = -\frac{GrB_7}{4m_8^2 + 4m_8 - \beta} \quad A_{12} = -\frac{GrB_8}{4m_6^2 + 4m_6 - \beta} \quad A_{13} = -\frac{GrB_9}{4m_2^2 + 4m_2 - \beta}$$

$$A_{14} = -\frac{GrB_{10}}{(m_6 + m_8)^2 + (m_6 + m_8) - \beta} \quad A_{15} = -\frac{GrB_{11}}{(m_2 + m_8)^2 + (m_2 + m_8) - \beta} \quad A_{16} = -\frac{GrB_{12}}{(m_2 + m_8)^2 + (m_2 + m_8) - \beta}$$

$$A_{17} = -(A_4 + A_5 + A_6 + A_7 + A_8 + A_9 + A_{10} + A_{11} + A_{12} + A_{13} + A_{14} + A_{15} + A_{16})$$

III. RESULTS AND DISCUSSION

The variation of non-dimensional velocity, temperature, concentration, skin friction, Nusselt number, Sherwood number for different values of Grashof number (Gr), Solutal Grashof number (Gc), Porosity permeability (K), Chemical reaction parameter (Kr), Magnetic parameter (M), Prandtl number (Pr), Heat source parameter (Q), Radiation parameter (R), Eckert number (Ec) and Schmidt number (Sc) are shown in figures (2) - (20). Figure (2) shows the influence of thermal buoyancy force parameter (Gr) on the velocity. As can be seen from this figure, the velocity profile increases with increases in the values of the thermal buoyancy. We actually observe that the velocity overshoot in the boundary layer region. Buoyancy force acts like a favourable pressure gradient which accelerates the fluid within the boundary layer therefore the solutal buoyancy force parameter (Gc) has the same effect on the velocity shown in figure (3). The effects of the viscous dissipation parameter i.e., the Eckert number (Ec) on the velocity profiles depicted in figure (4). It is clear that the velocity decreases with increases in Eckert number. Figure (5) displays that the velocity increases with a rise in permeability parameter (K). Moreover, for small permeability, the velocity reduces faster than when the permeability is higher. Figure (6) gives the velocity profiles for various values of chemical reaction parameter (Kr), it is evidence that velocity decreases with stronger chemical reaction parameter. Figure (7) reveals that velocity profiles decreases as magnetic parameter (M) increases. This may be attributed to the fact that an increase in magnetic parameter signifies an enhancement of Lorentz force, thereby reducing the magnitude of the velocity. This figure further indicates that blood velocity in the capillary decreases with increase in distance from the lower wall of the capillary. Figure (8) illustrates the effect of Prandtl number (Pr) on the velocity profiles. It is noticed that as the Prandtl number (Pr) increases, the velocity decreases. As seen in the earlier cases, far away from the plate, the effect is much significant. Figure (9) show the effect of radiation parameter (R) on the velocity profiles, it is observed that the velocity decrease as the radiation parameter increases. This result qualitatively agrees with expectations. Influence of Eckert number (Ec) on temperature distribution is displayed in figure (10). Here both the temperature and thermal boundary layer thickness decrease when Eckert number increases. In fact Eckert number is decreased due to more cool by friction and thus temperature profiles decreases. The temperature profiles for different values of thermal Grashof number and solutal Grashof number are show in figures (11) and (12); form these figures observe that an increases both the parameter the results are decreases. Figure (13) illuminates a very important effect of magnetic parameter (M) on the temperature profile. It is revealed that temperature field is higher values of magnetic parameter. Because with the increase of magnetic parameter the Lorentz force (which is a resistive force) increases and consequently more heat is produced. Hence temperature profiles increases. The temperature profiles for different values of chemical reaction parameter shown in figure (14), it is clear that an increases in chemical reaction parameter the temperature profiles decreases. Figure (15) is drawn to see the effect of Prandtl number (Pr) on temperature profiles. It is clearly shown that temperature profiles decreases when Prandtl number is increases. In fact higher Prandtl number fluid has low thermal diffusivity

which is responsible for the reduction of temperature profile. Figure (16) demonstrates the effects of radiation parameter (R) on the temperature distribution. It is analyzed that the higher values of radiation parameter decrease the temperature profiles and thermal boundary layer thickness. The effects of order of chemical reaction on concentration distributions are displayed in figure (17) respectively. It is observed from this figure that an increase in the chemical reaction leads to decrease the concentration profiles. Figure (18) illustrate the concentration profiles for different Schmidt number (Sc). An increase in Schmidt number the concentration profiles decreases. The skin friction for different values of radiation parameter (R) versus Grashof number (Gr) shown in figure (19), it is observed that an increases in radiation parameter decreases. The rate or heat transfer for different values of Prandtl number (Pr) versus Grashof number (Gr) shown in figure (20), it is clear that increases in Prandtl number the Nusselt number increases.

IV. CONCLUSIONS

Comparisons of the present results with previously published work on some limiting cases were performed and results were found to be in excellent agreement. From the present investigation following conclusions are drawn:

- Increasing the magnetic field parameter decreases the flow velocity near the stretching sheet in the momentum boundary layer, whereas its effect is reversed as the space variable of porous permeability parameter.
- Temperature decreases where as increases in radiation parameter.
- Skin friction increases with increase in the value of Soret number.
- Temperature decreases with increase in non-uniform heat source parameter
- Increase in the value of Schmidt number the concentration profiles decreases.

REFERENCES

- [1] A J Chamkha (2003): MHD flow of a Numerical of uniformly stretched vertical permeable surface in the presence of heat generation/absorption and a chemical reaction, *Int. Comm. Heat Mass Transfer*, Vol. 30, pp. 413-422
- [2] A Y Ghaly and E M E Elbarbary (2002): Radiation effect on MHD free convection flow of a gas at a stretching surface with a uniform free stream, *J. Appl. Math.* Vol. 2 (2), pp. 93-103
- [3] Chien – Hsin – Chen (2004): Combined heat and mass transfer in MHD free convection from a vertical surface with ohmic heating and viscous dissipation. *Int. J. Engng. Sci.* Vol. 42 (7), pp. 699-713
- [4] D Ch Kesavaiah, P V Satyanarayana and S Venkataramana (2011): Effects of the chemical reaction and radiation absorption on an unsteady MHD convective heat and mass transfer flow past a semi-infinite vertical permeable moving plate embedded in a porous medium with heat source and suction, *Int. J. of Appl. Math and Mech.* Vol. 7 (1), pp. 52-69
- [5] E M A Elbashedy (1997): Heat and Mass transfer along a vertical plate with variable temperature and concentration in the presence of magnetic field. *Int. J. Engng. Sci.* Vol. 34, pp. 515-522
- [6] E M Aboeldahab and E M E Elbarbary (2001): Hall current effect magneto hydrodynamics free convection flow past a semi infinite vertical plate with mass transfer, *Int. J. Engng. Sci.* 39, pp. 1641–1652
- [7] F S Ibrahim, A M Elaiw and A A Bakr (2008): Effect of the chemical reaction and radiation absorption on the unsteady MHD free convection flow past a semi-infinite vertical permeable moving plate with heat source and suction, *Communications in Non-linear Science and Numerical Simulation*, Vol. (13), pp. 1056-1066
- [8] M A Hossain (1992): Viscous and Joule heating effects on MHD free convection flow with variable plate temperature. *Int. J. Heat Mass Transfer.* Vol. 35, pp. 3485-3487
- [9] M A Hossain and D A S Rees (1999): Combined heat and mass transfer in natural convection flow from a vertical wavy surface. *Acta Mechanica.* Vol. 136, pp. 133-141
- [10] M A Hossain, M A Alim and D A S Rees (1999): The effect of radiation on free convection from a porous vertical plate, *Int. J. Heat Mass Transfer.* Vol. 42, pp. 181 -191
- [11] M Acharya, G C Dash and L P Singh (2001): Hall Effect with simultaneous thermal and mass diffusion on unsteady hydromagnetic flow near an accelerated vertical plate. *Ind. J. Physics. B.* Vol. 75B (1), pp. 68–70
- [12] M Bhavana, D Chenna Kesavaiah and A Sudhakaraiah (2013): The Soret effect on free convective unsteady MHD flow over a vertical plate with heat source, *International Journal of Innovative Research in Science, Engineering and Technology*, Vol. 2 (5), pp. 1617-1628
- [13] N Datta and R N Jana (1976): Oscillatory magnetohydrodynamic flow past a flat plate with Hall effects, *J. Phys., Soc. Japan.* Vol. 40, pp.1469-1475
- [14] O Aydin and A Kaya (2008): Non - Darcian forced convection flow of viscous dissipating fluid over a flat plate embedded in a porous medium. *TRANS POROUS MEDIA.* Vol. 73 (2). pp.173–186
- [15] O Aydin and A Kaya (2009): MHD mixed convection of a viscous dissipating fluid about permeable vertical flat plate. *Appl. Math. Model.* Vol. 33 (110), pp. 4086–4096

- [16] P Ganesan and G Palani (2004): Finite difference analysis of unsteady natural convection MHD flow past an inclined plate with variable surface heat and mass flux. *Int. J. of Heat and Mass Transfer*, Vol. 47 (19-20), pp. 4449–4457
- [17] P Ganesan and G Palani (2004): Numerical solution of unsteady MHD flow past a semi-infinite isothermal vertical plate, *Proceedings of the 6th ISHMT/ASME Heat and Mass Transfer Conference and 17th National Heat and Mass Transfer Conference*, January 5–7, 2004, Kalpakkam, India, pp. 184–187
- [18] R A Mohamed (2009): Double – Diffusive Convection radiation interaction on unsteady MHD flow over a vertical moving porous plate with heat generation and Soret effects, *Appl. Math. Sci.*, Vol 3 (13), pp. 629-651
- [19] R Muthucumaraswamy and P Ganesan (2001): Effect of the chemical reaction and injection of flow characteristics in an unsteady upward motion of an isothermal plate. *J. Appl. Mech. Tech. Phys*, Vol. 42, pp. 665-671
- [20] R Muthukumaraswamy and G K Senthil (2004): Heat and mass transfer effects on moving vertical plate in the presence of thermal radiation. *Theoret, Appl. Mech.* Vol. 31 (1), pp. 35-46
- [21] Rita Choudhury and Sajal Kumar Das (2013): Mixed Convective Visco-Elastic MHD Flow with Ohmic Heating, *International Journal of Computer Applications* (0975 – 8887) Vol. 68 (10), pp.7-13
- [22] V S H Babu and G V R Reddy (2011): Mass transfer effects on MHD mixed convective flow from a vertical surface with ohmic heating and viscous dissipation. *Advances in Appl. Sci. Res.* Vol. 2 (4), pp. 138-146

FIGURES:

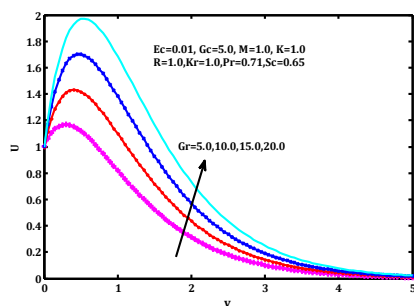


Figure (2): Velocity profiles for different values of Gr

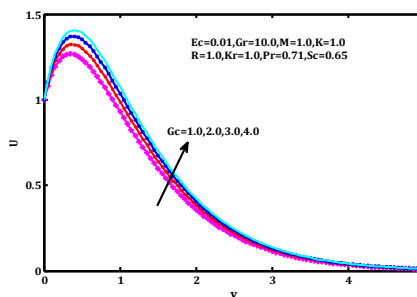


Figure (3): Velocity profiles for different values of Gc

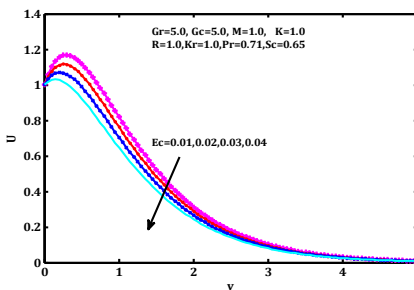


Figure (4): Velocity profiles for different values of Ec

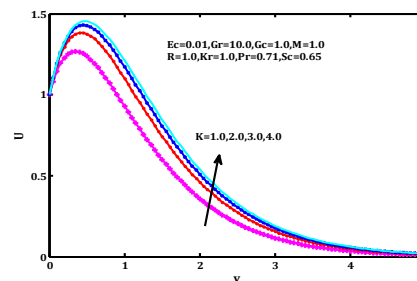


Figure (5): Velocity profiles for different values of K

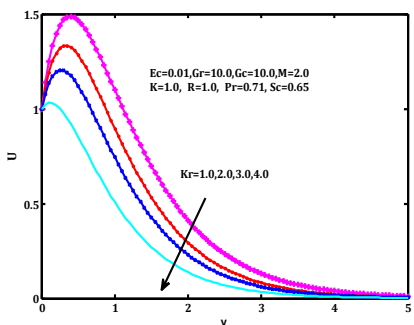


Figure (6): Velocity profiles for different values of Kr

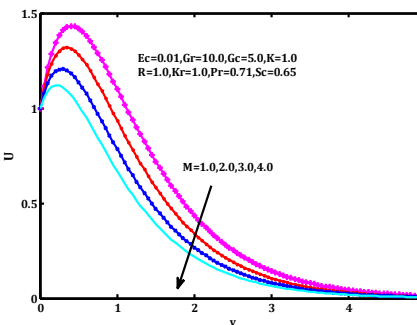


Figure (7): Velocity profiles for different values of M

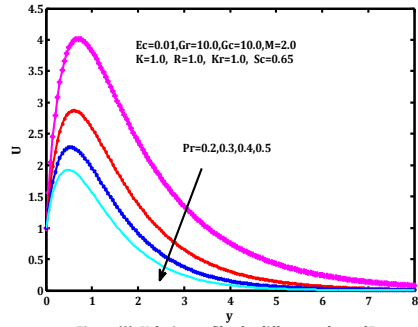


Figure (8): Velocity profiles for different values of Pr

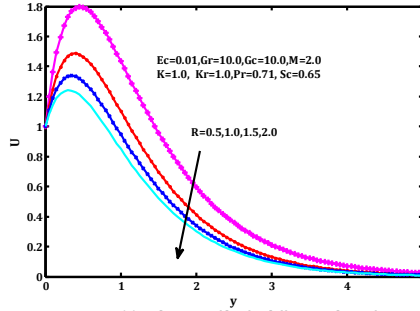


Figure (9): Velocity profiles for different values of R

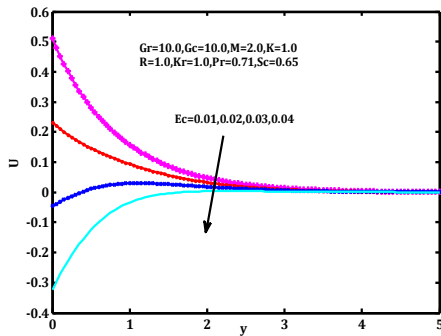


Figure (10): Temperature profiles for different values of Ec

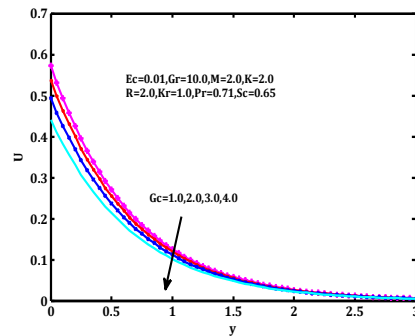


Figure (11): Temperature profiles for different values of Gc

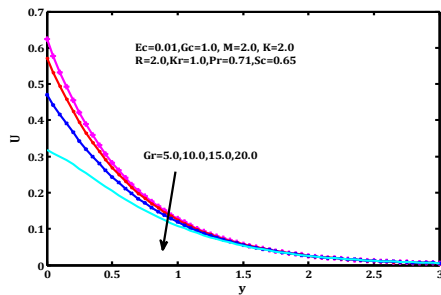


Figure (12): Temperature profiles for different values of Gr

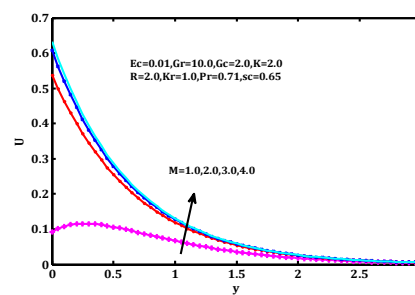


Figure (13): Temperature profiles for different values of M

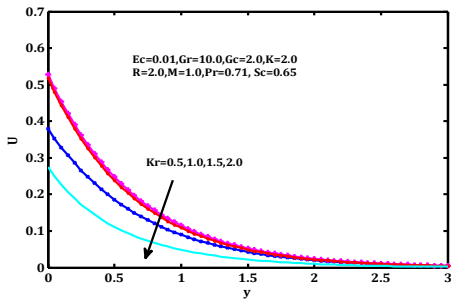


Figure (14): Temperature profiles for different values of Kr

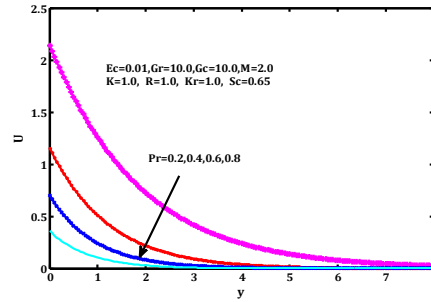


Figure (15): Temperature profiles for different values of Pr

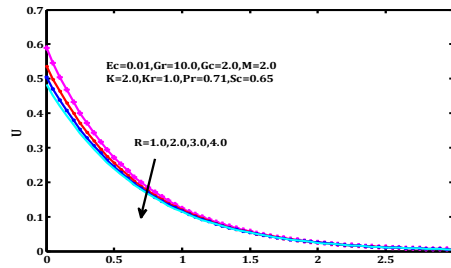


Figure (16): Temperature profiles for different values of R

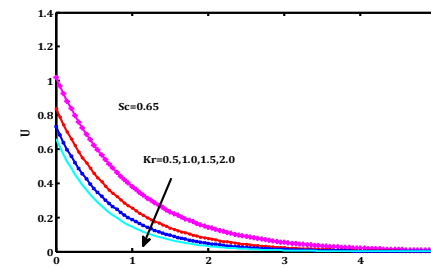


Figure (17): Concentration profiles for different values of Kr

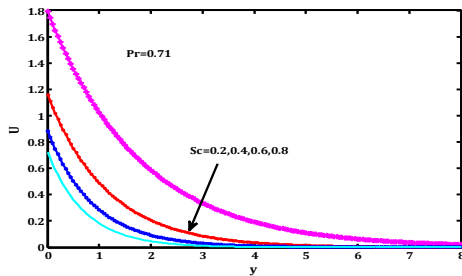


Figure (18): Concentration profiles for different values of Sc

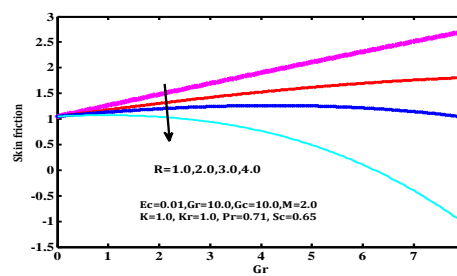


Figure (19): Skin friction for different values of R versus Gr

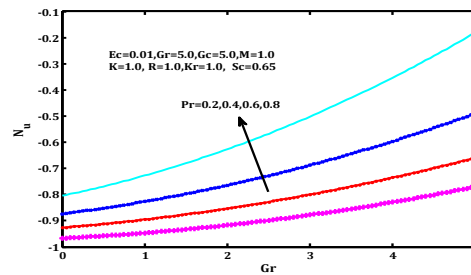


Figure (20): Nusselt number for different values of Pr versus Gr